

## Author Manuscript

### Published in final edited form as:

*The Computational Mechanics of Bone Tissue*, Lecture Notes in  
Computational Vision and Biomechanics 35. (2020) 179 – 202

Doi: 10.1007/978-3-030-37541-6\_7

### Title:

#### Finite Element Analysis of Bone and Experimental Validation

*Francisco M. P. Almeida and António M. G. Completo\**

<sup>1</sup> Department of Mechanical Engineering, University of Aveiro, Portugal

**Corresponding Author:** \*António Completo. Email: [completo@ua.pt](mailto:completo@ua.pt)

## **Abstract**

This chapter describes the application of the finite element (FE) method to bone tissues. The aspects that differ the most between bone and other materials' FE analysis are the type of elements used, constitutive models, and experimental validation. These aspects are looked at from a historical evolution stand point.

Several types of elements can be used to simulate similar bone structures and within the same analysis many types of elements may be needed to realistically simulate an anatomical part.

Special attention is made to constitutive models, including the use of density-elasticity relationships made possible through CT-scanned images. Other more complex models are also described that include viscoelasticity and anisotropy.

The importance of experimental validation is discussed, describing several methods used by different authors in this challenging field. The use of cadaveric human bones is not always possible or desirable and other options are described, as the use of animal or artificial bones. Strain and strain rate measuring methods are also discussed, such as rosette strain gauges and optical devices.

## 1. Introduction

Probably the first ever published work on finite element (FE) analysis in the field of biomechanics was the article of Brekelmans et al (1972). They developed a two dimensional FE model of a human femur. The bone was considered a homogeneous, isotropic and linear material with a Young's modulus of 20 GPa and a Poisson's ratio of 0.37. Brekelmans et al divided the model into 936 triangular elements and subjected it to very simple forces and boundary conditions, what by today standards could be considered extremely simple and basic.

However, the biomechanical study of bone did not start there. Before that, many researchers dedicated their time to studying mechanical properties of anatomical parts, especially bone. It is reported that Galileo published work on bone mechanics as early as 1638 (Ascenzi, 1993), and it is known that this has been the subject matter of many studies since then.

By 1983 Huiskes and Chao (1983) reported about the first ten years of FE analysis in biomechanics. They were optimistic about the evolution of the field, especially in view of developments in mechanical engineering and the rapid evolution of computers. Their main concerns were in understanding the complexity of clinical problems and the behaviour of biological structures. They considered that after the acquisition of this knowledge, its correct implementation into an FE analysis was also a major hurdle to overcome in the field of biomechanics.

From then on, the FE analysis of bone has been evolving in an almost exponential way. If original studies were in two dimensions, whether in plain stress or axisymmetric, and constitutive models were simple isotropic linear elastic, present studies are easily performed in three dimensions and constitutive models can be very complex as will be described later in this chapter. The number of elements in an FE model is also representative of this evolution, while in the 1980s these were counted by the hundreds, today FE models can certainly have more than 100,000 elements (Taylor & Prendergast, 2015). Recently, two noteworthy articles were published reporting on the first four decades of FE analysis applied to biomechanics, the first one on lumbar intervertebral discs (Schmidt, et al., 2013), the other on orthopaedic devices (Taylor & Prendergast, 2015). Both articles' tone is one that conveys the advanced state of a field that has proved its value, but also has some new challenges like accounting for patient variability and other uncertainties.

The implementation of an FE analysis requires several inputs. Including geometry, element type, constitutive models of materials, meshing considerations, boundary conditions and loading, verification and validations. Bone FE analyses, as any other FE analysis, require all these data. However, the parts that raise more questions and differ the most from other types of FE analysis are the types of elements, constitutive models and validation. For these reasons these will be the topics discussed in this chapter.

## 2. Element Types

During the process of creating an FE model choices have to be made regarding the type of element representing diverse parts of the structure being studied. This choice is related with various factors including but not limited to:

- Type of analysis, e.g. 2D, axisymmetric, 3D;

- Geometry, whether it is simple or complex, or can be simplified;
- Expected behaviour, e.g. small deformations or large deformations;
- Constitutive model, some element types may not be compatible with some constitutive models.

There are innumerable types of elements, each with its specific mathematical model, nonetheless there are some types of elements that fall within the same set of basic properties. Biomechanics can be a quite demanding field in this regard, within the same analysis one can easily find several types of elements. What follows does not aim to be a detailed description of the elements used by the referred authors, which is absent in the published articles most of the times, but rather a general view of different approaches to similar problems regarding bone tissue discretization.

When modelled in three dimensional studies, both cortical and cancellous bone are most times represented through hexahedral, eight-node elements, e.g.: (Kumaresan, et al., 1999), (Zander, et al., 2001), (Schmidt, et al., 2007), (Papaioannou, et al., 2008), (Faizan, et al., 2009), (Wolfram, et al., 2010), (Zhang, et al., 2011), (Niemeyer, et al., 2012), (Kinzl, et al., 2013), (Liu, 2014), (Lughmani, et al., 2015). Although with some disadvantages related to accuracy and excessive stiffness (Donald, 2011) (Burkhart, et al., 2013), four-node tetrahedral elements are sometimes used for modelling cortical and cancellous bone because they are very easy to use in complex geometries, e.g.: (Gu & Li, 2011), (Evans, et al., 2012), (Hussain, et al., 2012), (Parr, et al., 2013). As a means to overcome first-order tetrahedral elements' disadvantages, in some studies cortical and cancellous bone are modelled through second-order (ten-node) tetrahedral elements, e.g.: (Taddei, et al., 2006) (Austman, et al., 2008), (Nazemi, et al., 2015).

In some FE analyses cancellous bone and cortical bone are modelled with distinct elements, as is the case in Denozière and Ku (2006) and Ezquerro et al (2011), where cortical bone was represented through hexahedral elements, and cancellous bone was represented through tetrahedral elements. In other instances 3D solid elements (hexahedral or tetrahedral) are used for cancellous bone, while shell elements are used for cortical bone, e.g.: (Beillas, et al., 2007), (Bowden, et al., 2008), (Little & Adam, 2011), (Dong, et al., 2013), (Wang, et al., 2013).

Stiffness of bones is several orders of magnitude higher than soft tissues' stiffness. For this reason, in some types of analyses, the error committed by considering bones as rigid structures is small. Several authors have opted for this solution, therefore saving computer processing time, e.g.: (Bendjaballah, et al., 1995), (Moglo & Shirazi-Adl, 2003), (Donahue, et al., 2003), (Ramaniraka, et al., 2005), (Peña, et al., 2006), (Li, et al., 2009), (Rohlmann, et al., 2010), (Yue-fu, et al., 2011).

### **3. Constitutive Models of Bone**

The choice of constitutive models to represent different bony tissues depends on many factors. Along the history of FE analysis in biomechanics there has been a noticeable evolution in complexity of these models, resulting from the increasing understanding of tissues' behaviour and simultaneously the rapid progress in computing power. As all but the simplest models can be described by a restrict set of parameters, a comprehensive analysis on the development of constitutive models would be very incomplete without a short description of its implementation. Many models overlap in some aspects, most are not totally original and build on previously developed ones. The selection of constitutive models presented here seeks to display original studies and their evolution through subsequent works.

Bone has been a deeply studied material within the subject of biomechanics. Besides the consequences of malformations and diseases such as osteoporosis, its constitutive model is very important in the field of orthopaedic surgery. In many types of surgeries, bone is the primary material to which implants and screws are attached. For these reasons there are great quantities of FE studies that must take in consideration an appropriate constitutive model of bone.

Most bones are composed of two forms of bone tissue. Cortical bone constitutes the structural shell of nearly all bones. Cancellous bone is contained within cortical bone and forms a continuous mass, made of a three-dimensional lattice comprising rod like and plate like portions, the trabeculae. The compactness of the trabeculae defines the level of porosity and density of cancellous bone. By definition cancellous bone exhibits a relative density varying from 0.05 to 0.7, while cortical bone shows a relative density between 0.7 and 0.95, where relative density is the ratio of specimen density to that of fully dense cortical bone. Cortical bone shows a porosity of approximately 5 to 30 percent and the porosity of cancellous bone varies between approximately 30 and 90 percent. Apparent density is another important parameter defined by the mineralized mass divided by total tissue volume. It can be used for measuring mechanical properties of bone and shows an almost linear relation with porosity (Carter & Hayes, 1977) (Cowin, 2001) (Mow & Huiskes, 2005).

Bone tissue is composed of cells surrounded by a matrix. This matrix consists mainly of collagen (mostly type I) and a mineral phase (mostly calcium phosphate and calcium carbonate). Most of this mineral phase is arranged in hydroxyapatite crystals which are the main source of bones rigidity (Cowin, 2001) (Mow & Huiskes, 2005). This composition and variability does not result in a simple constitutive model, as can be seen by the work of many researchers.

The understanding of this complex behaviour has been increasing throughout history. Testing on several types of human bones Dempster and Liddicoat (1952) found that cortical bone was non-isotropic and showed inelastic behaviour before the breaking point. For the longitudinal direction their measured values of Young's moduli were on average 2.5 and 3.0 million psi (17.2 and 20.7 GPa) for dry bone, in tension and compression respectively; for wet bones the values obtained were lower by about 0.5 million psi (3.4 GPa) in compression and 1 million psi (6.9 GPa) in tension. Adding to this, for radial and tangential directions the values obtained were both 52% of the modulus for the longitudinal direction. In the same study Dempster and Liddicoat also measured the ultimate compressive strength, obtaining values for the longitudinal direction in the order of 25,000 psi (172 MPa) for dry bone, and 15,000 psi (103 MPa) for wet bone, and slightly lower values for transverse directions.

Throughout their study, Dempster and Liddicoat compared the mechanical properties of bone with that of other materials such as wood, concrete and steel. They go further to say that in many respects bone exhibits a similar behaviour to wood, in part because both materials present mainly orthotropic mechanical properties.

In most FE studies bone is considered a linear elastic isotropic time-independent material. This constitutes a pronounced simplification, especially in the case of cancellous bone where several studies have been trying to implement more complex models with varying site specific properties. In the case of cortical bone its inherent anisotropy is the major issue. Considering simpler models represents an advantage in terms of model construction and computational resources, but there are instances where it is necessary or advantageous to use more complex representations than can replicate more accurately the reality.

Brekelmans et al (1972) completely ignored the distinction between cancellous and cortical bone, and for their 2D FE analysis of a human femur, a homogenous, isotropic, linear elastic model was used. They applied a Young's modulus of 20 GPa and a Poisson's ratio of 0.37.

In another early instance of FE analysis applied to the field of biomechanics, Huiskes et al (1981) studied the behaviour of a human femur, considering the cortical material linear elastic, homogeneous and transversely isotropic. Again, cancellous material was not considered. Even so, they found excellent agreement with experimental results. Huiskes et al considered that FE analysis were able to accurately represent at least the diaphysis of the femur. In the same study an axisymmetric FE analysis of the femur was performed. The values for the Young's moduli considered were 20 and 13.6 GPa for the longitudinal and transverse directions respectively, and Poisson's ratio was taken as 0.37.

In one timely attempt to capture cancellous bone variability and complexity, Brown and Ferguson (1980) tested large numbers of 5 mm edge length cubic specimens of human proximal femur cancellous bone in three orthogonal directions. Their results showed the markedly anisotropic behaviour of this structure but also a clear proportionality between Young's modulus and yield strength, independent of direction. The values for the elasticity modulus obtained were rather high ranging from 1 GPa to 9.7 GPa; yield strengths measured fell between 120 and 310 MPa.

Adapting the available information about cancellous bone to FE analysis, Taylor et al (1995) used a very simple FE model of the femoral part of a hip prosthesis with all materials considered homogenous, isotropic and perfectly elastic for the exception of cancellous bone which was considered elastic perfectly plastic. This was done as an attempt to gain a better understanding of the interface between bone and implant.

Kopperdahl and Keaveny (1998) proposed that tensile yield strain of cancellous bone is independent of apparent density for human bone, while compressive yield strains have a linear relation with apparent density. For vertebral cancellous bone, Kopperdahl and Keaveny arrived at the following average values: Young's modulus in compression and tension respectively = 291 and 301 MPa; yield strain in compression and tension respectively = 0.84 and 0.78%; ultimate strain in compression and tension respectively = 1.45 and 1.59%; yield stress in compression and tension respectively = 1.92 and 1.75 MPa; ultimate stress in compression and tension (equal) = 2.23 MPa.

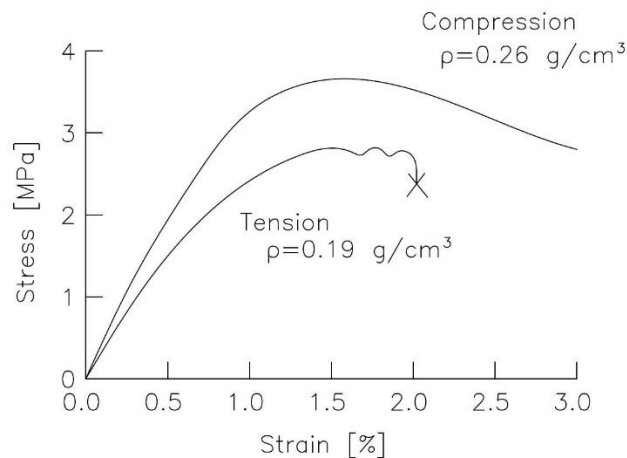


**Fig. 1** Typical stress-strain behaviour of cancellous bone of different densities, adapted from (Kopperdahl & Keaveny, 1998).

Morgan and Keaveny (2001), through the analysis of several specimens of cancellous bone from four anatomical sites, found that both yield strain and stress could be better predicted when a site specific model was adopted. It was hypothesised that this had to do with the particular architecture and hard tissue properties of cancellous bone at those sites. On the same subject Chang et al (1999) found yield strains of cancellous bone to be isotropic. Studying on bovine cancellous bone, characterized by high density and strong plate like anisotropic architecture, Chang et al found that this bone showed similar yield strains between on-axis and 90° off-axis. From the particular characteristics of these bones, they made extrapolations to other bones, including human. In reality bone can be said to have an anisotropic viscoelastic behaviour, which is adequately simplified for most studies. However, Iyo et al (2004), considering that the viscoelastic anisotropy was important for implant fixations, proposed a model from which the Young's modulus of cortical bone could be derived as a function of time. Such a study can serve as an example of how complex the description of bone's constitutive model can be.

### 3.1 Use of CT-Scans and Density-Elasticity Relationship

Because mechanical properties of bone vary tremendously, there has been a stimulus to create FE models that reflect these changing values from element to element. The relation between bone density and its mechanical properties has been known for quite some time (Galante, et al., 1970) (Carter & Hayes, 1977) (Lotz, et al., 1990) (Hodgskinson & Currey, 1992) (Kalender, et al., 1995) (Rho, et al., 1995) (Wirtz, et al., 2000). In the last fifteen years it has been possible to apply this relationship to FE models, mostly by making use of values acquired through Quantitative Computed Tomography scanning (QCT). These models have been increasing in complexity with the improvement of imaging technologies and computer power.

QCT is a technique that allows the measurement of bone density using Computed Tomography (CT) scanners calibrated through the use of phantoms, such as the European Spine Phantom (ESP) (Adams, 2009). The ESP was created in 1995 and its original purpose was to calibrate CT scanners and DXA devices in order to obtain correctly evaluated diagnoses of osteoporosis regardless of where the exam was performed (Kalender, et al., 1995). However, as for QCT in general, its use proved extremely useful in FE bone analysis, as it allowed increasing confidence in the collected data.

Most studies try to match the relationship between a mechanical property and bone density through an empirical equation of the form (Carter & Hayes, 1977):

$$\gamma = A \rho^B$$

Where  $\gamma$  is the material property (mostly Young's modulus or strength),  $\rho$  is the apparent density, and A and B are experimentally derived constants.

Galante et al (1970) defined two different densities regarding cancellous bone: apparent density that equals the weight divided by the total volume of the sample and real density that is equal to the weight divided by the volume of the matrix excluding the marrow vascular spaces. They tested samples from human lumbar vertebrae under compression. Their results showed very good relation between apparent density and compressive strength, obtaining the following equation:

$$Y = -6.9 + 128.02 X$$

Where Y is the strength in  $\text{kp/cm}^2$ , and X is the apparent density in  $\text{g/cm}^3$ .

Galante et al proposed that apparent density was more important than real density in the evaluation of strength of cancellous bone. In their study, time dependent and anisotropy results were also noticed, leading them to suggest that cancellous bone has a complex rheological behaviour.

Using samples of human and bovine cancellous bones, Carter and Hayes (1977) arrived at the following relationship:

$$E = 3790 \varepsilon_r^{0.06} \rho^3$$

Where E is the Young's modulus in MPa,  $\varepsilon_r$  is the strain rate in  $\text{s}^{-1}$ , and  $\rho$  is apparent density in  $\text{g/cm}^3$ .

Lotz et al (1990) studied the relationship between human proximal femur cancellous bone apparent density and mechanical properties. The samples were initially scanned using QCT, then mechanical properties were measured and finally the density was experimentally measured. This process permitted establishing a direct relation between QCT data and mechanical properties. They obtained highly positive correlations with compressive Young's modulus and also with compressive strength through the following equations:

$$E = 1310 \rho^{1.40}$$

$$\sigma = 25 \rho^{1.8}$$

Where E is the Young's modulus in MPa,  $\rho$  is the apparent density in  $\text{g/cm}^3$  and  $\sigma$  is the compressive strength in MPa.

Hodgskinson and Currey (1992) studied the relationship between density and Young's modulus for a wide variety of cancellous bone types, corresponding to a wide range of densities. They found a very strong correlation for the entire interval even when considering bones from different species such as human, equine and bovine.

Having FE analysis in mind and trying to overcome the fact that density-elasticity ratios do not provide any information regarding the anisotropy of bones, Rho et al (1995) provided a series of orthotropic ratios between measured density and Young's modulus for several human bones. In their equations axial elasticity is a function of density, while radial and circumferential elasticity are functions of axial elasticity. These relationships were found to be stronger for cancellous bone than for cortical bone.

By means of a meta-analysis of literature, Wirtz et al (2000) provided a very comprehensive study of this type of relationships. At an early stage of this method, Wirtz et al described that each finite element can be characterized by its QCT derived apparent density. For both cortical and cancellous bone, relations between density and Young's modulus, strength, shear modulus, Poisson's ratio and viscoelastic behaviour were provided as follows.

Young's modulus (E) in MPa – apparent density ( $\rho$ ) in  $\text{g/cm}^3$  relationships for cortical femoral bone in the axial and transverse direction respectively:

$$E = 2065 \rho^{3.09}$$

$$E = 2314 \rho^{1.57}$$



Young's modulus – apparent density relationships for cancellous femoral bone in the axial and transverse direction respectively:

$$E = 1904\rho^{1.64}$$

$$E = 1157\rho^{1.78}$$

Compressive strength ( $\sigma_b$ ) – apparent density relationships for cortical femoral bone in the axial and transverse direction respectively:

$$\sigma_b = 72.4\rho^{1.88}$$

$$\sigma_b = 37\rho^{1.51}$$

Compressive strength – apparent density relationships for cancellous femoral bone in the axial and transverse direction respectively:

$$\sigma_b = 40.8\rho^{1.89}$$

$$\sigma_b = 21.4\rho^{1.37}$$

For Poisson's ratio Wirtz et al offered average values of 0.3 for cortical bone and 0.12 for cancellous bone.

Regarding viscoelasticity, Wirtz et al referred to the formula of Carter and Hayes (1976) where  $\varepsilon_r$  equals the strain rate in  $s^{-1}$ :

$$\sigma_b = 68\varepsilon_r^{0.06}\rho^2$$

Taylor et al (2002) derived the orthotropic elastic constants of a human femur by comparing experimentally measured natural frequencies with values obtained through an FE modal analysis. The model used for the FE construct resulted from CT scan data where an orthotropic density–elasticity relation was used and applied to each element as a function of its position along 16 different radial orientations. The three different Young's modulus and shear modulus equations were a function of density and of a maximum value for each modulus. Through the use of an FE modal analysis Taylor et al were able to validate the entire bone model instead of site specific values acquired through strain gauges.

As an example of application of density–elasticity relation to a specific problem, Pancanti et al (2003) used the equations derived by Wirtz et al (2000) in order to obtain a more precise FE model of a cementless total hip replacement.

When there was already some accumulated experience regarding the application of CT scanned data to FE models, Taddei et al (2004) presented a very clear set of possible ways to implement this technique:

- From the simpler 'voxel mesh' where cubic elements were generated from the information contained in a pre-set number of voxels. The constitutive model of each element being derived from the average density of the voxels that fall within it.

- Through the use of a structured mesh, where facets of elements could be made to coincide with tissue boundaries. Similarly to the above described method, each element properties were derived from an average of the measured densities within it. The major disadvantage of this method being that some manual input was needed when defining the mesh geometry.
- Using an unstructured mesh, in which case there is no alignment of element facets with tissue boundaries. This procedure relies in a more automated approach since it becomes impossible to manually define element properties, but ultimately also depends on averaging densities within each element in order to derive its mechanical properties.

Additionally, Taddei et al presented a software that improves the automatization of this process, mapping CT scanned data into FE models. With increasingly more expedite processes a trend starts to unravel towards the use of patient-specific models, allowing the study of interventions that account for specific bone characteristics of each individual.

Morgan et al (2003) studied different density-elasticity ratios obtained for cancellous bone from different anatomical sites. By investigating cancellous bone from vertebra, proximal tibia, femoral greater trochanter and femoral neck, they concluded that the axial elasticity-density ratio for cancellous bone varied depending on the anatomical site under study. Using the same type of mathematical relationship presented above (Carter & Hayes, 1976) (Lotz, et al., 1990) (Wirtz, et al., 2000), they derived several equations to account for this variation. Morgan et al attributed the varying relationships to differences in local cancellous bone architecture.

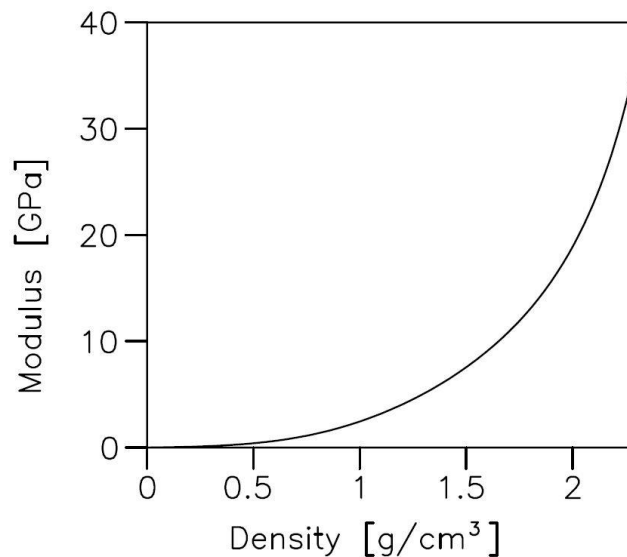


**Fig. 2** Typical density-elasticity relationship, adapted from (Laz, et al., 2007)

Taddei et al (2006), using data from a CT scanned femur, constructed two FE models. In the first case a different Young's modulus was attributed to each element, based on the average density, numerically integrated through the element's volume and using the following formula:

$$E = 10.5\rho_{ash}^{2.29}$$

Where  $\rho_{ash}$  is ash density. The application of this method provided a maximum Young's modulus of 19.8 GPa and a 12.9 GPa average for cortical bone.

For the second model only two discrete material models were used. Applying the above equation, a calibrated homogeneous Young's modulus value of 19.3 GPa was arrived at for cortical bone and 590 MPa for cancellous bone. Cortical and cancellous bone were distinguished at a predefined threshold density value from the CT data.

While both models correlated well with experimental values obtained for the same bone, the first method proved more accurate. Taddei et al considered that it is possible to use automatic tools to generate FE models from CT data, and that accuracy is influenced by the material models mapping strategy implemented.

In order to overcome some of the shortcomings resulting from considering isotropy for the whole bone model, Marangalou et al (2013) used the data obtained from micro-CT scans to attribute a site varying orthotropic model to cancellous bone. Clinical CT-scans do not have enough resolution to detail the microstructure of cancellous bone and by simply applying a density-elasticity ratio, errors are made, whether by over or under estimation of mechanical properties, depending on direction. Their micro-CT derived orthotropic model showed higher correlation with micro-CT measurements than other isotropic models. Marangalou et al considered that this approach can lead to more precise estimates of strength and elasticity of osteoporotic bones, and around implants for surgery studies.

In order to study the evolution of osteoarthritis in subchondral proximal tibia, Nazemi et al (2015) evaluated several density-elasticity equations (Morgan, et al., 2003) (Rho, et al., 1995) (Hodgskinson & Currey, 1992) comparing the results of FE analyses with macro indentation tests. They concluded that for this particular anatomical area no single equation offered a good prediction of mechanical properties, and underlined the importance of accounting for bone's heterogeneity when performing this type of FE studies.

### **3.2 Micro Finite Element Modelling**

The first time a micro FE model of a bone was attempted was more than two decades ago, requiring the use of supercomputers (Rietbergen & Ito, 2015). Nowadays, with improvements in imaging technology, models with higher degree of definition have been made easier to create. In particular, high-resolution peripheral quantitative CT (HR-pQCT) is a technology that has been enabling the study of the micro-structure of peripheral bones in-vivo.

This technology has been mostly used to predict the strength of bones as a diagnostic tool in cases of osteoporosis and other bone affecting diseases. This technique enables the acquisition of bone micro-structure, which can afterwards be studied using the effective Young's modulus, as opposed to the apparent Young's modulus, used in most analyses. In the future this technology will probably be available to anatomical parts other than peripheral bones (in-vivo), in which case other applications may arise, such as an aid in complex orthopaedic surgeries.

In most cases of micro-FE analysis derived from HR-pQCT, a voxel conversion approach is utilized. In such studies, bone tissue voxels are converted into brick elements of the same size, while voxels indicative of soft tissues are ignored (Rietbergen & Ito, 2015).

In order to evaluate which density-elasticity model better predicted the behaviour of a whole human ulna, Austman et al (2008) applied different equations (Carter & Hayes, 1977) (Wirtz, et al., 2000) (Morgan, et al., 2003) (Lotz, et al., 1990) to a micro-FE model and compared it with experimental results. They concluded that the equation that showed the best match varied with specimen, but overall, Morgan et al (2003) and Carter and Hayes's (1977) equations were the ones that showed smaller errors.

In a similar study, Scholz et al (2013) compared different density-elasticity relationships (Carter & Hayes, 1977) (Morgan, et al., 2003) in an FE modal analysis of pelvic bone specimens with results obtained experimentally. They used micro-CT scanned data to construct micro-FE models. All of the density-elasticity relationships used had been acquired from long bones' models, so there were doubts regarding their adequacy to the pelvic bone, as the cortical layer of this bone is thinner. Scholz et al concluded that all the analysed FE models lacked stiffness, and the one that showed best results was the one using Morgan et al (2003) equations.

Liu et al (2010) compared the results of human distal tibial bones' models acquired through HR-pQCT with models acquired through micro-CT. Micro-CT is a technology considered the gold standard for this type of image acquisition, but cannot be practiced in-vivo, much less in humans. They concluded that the results showed high correlation, although HR-pQCT overestimated the mechanical properties of the bone. This may be the result of the combination of voxel size and density threshold utilised, because while micro-CT captures smaller details, HR-pQCT compensates for this by attributing a lower density value for each structural element; the result being thicker structures with lower Young's moduli, which at a global level ends up as a stronger and stiffer bone.

### 3.3 Complex Constitutive Models

As can be inferred by what has been described so far, the two main parts of bones, cortical and cancellous, are very different in their structure. For this reason, in general, even the simplest FE studies take into account two different models describing these two different regions. From a structural stand view it seems quite obvious that cortical bone is the most important part, however, the question may be posed in terms of how important cancellous bone is to the overall strength and stiffness. Different authors propose different methods that span from studying cancellous bone's resistance separately to considering that for some purposes, bone can safely be studied ignoring cancellous bone entirely.

A good example of this duality is the study of Parr et al (2013) where six different models of a human talus bone were considered, each one with differing levels of complexity. Starting from images acquired through micro-CT they were able to model the small intricacies of cancellous bone. Comparing the most realistic model, which included the micro-structure of cancellous bone and porosity in cortical bone, with other simpler models that deleted the cancellous bone or treated it as a homogeneous mass, the authors were able to measure the contribution of this interior network shaped structure to the overall stiffness of bone. They concluded that the way cancellous bone was modelled had a great impact on the stiffness of the whole bone. Other secondary but interesting point shown by their study was the importance of the computational development in this field: contrary to studies conducted one or two decades prior, this one was performed on a commercial desktop computer, taking at most one hour to analyse the most complex model.

One of the more complex constitutive laws for cortical bone was developed by Carnelli et al (2010) and Carnelli et al (2011). In these studies, they developed a model that accounts for anisotropic elastic and post-yield behaviour, as well as tension-compression mismatch and direction dependent yield stresses. They tested this model against nanoindentation experiments which they confirmed to show high correlation in most parameters. Carnelli et al advocate that such a complex model would help gaining a deeper knowledge of the microstructural behaviour of cortical bone tissue.

Contrary to the general trend, Koivumaki et al (2012), using models obtained through a multi-detector CT scanner, showed that the failure load of the proximal femur could be well predicted

by ignoring cancellous bone. In their FE models only the cortical part was considered, which allowed great savings in computer resources, and the results showed high correlation with experimental data, and only slightly worse results than a similar model where cancellous bone had been considered. Cortical bone was modelled using a bi-linear elastoplastic constitutive law, where the post-yield modulus was 5% of the initial elastic modulus. Failure was considered to occur when the material reached a stress of 118.6 MPa in tension or 1.35% strain in compression.

In order to include plasticity and damage control with a relatively simple constitutive model, Kinzl et al (2013) identified a crushable foam model that could be adapted to different bones and densities using only three different parameters. In their study they used QCT generated images where each voxel corresponded to an element. The major disadvantage of this material model was the absence of anisotropy, but when compared with other more complex and harder to implement models, Kinzl et al found that this readily available and easy to implement model showed similar results and was a good predictor of bone strength and damage.

With the objective of studying the region of interest during a pull-out of a pedicle screw from a vertebra, Liu et al (2014) used polyurethane foam as a substitute for cancellous bone and made an FE analysis where some of the material model parameters were changed in order to simulate different stages of osteoporosis. The experiments with polyurethane foam served for initial calibration of the FE model, which was subsequently used to gain a better understanding of the surrounding mechanics of a pedicle screw pull-out.

Concerning the study of cancellous bone at the interface with a press-fit proximal tibia implant, Nelly et al (2013) used a crushable foam with isotropic hardening model to improve the plastic deformation prediction. This type of model revealed superior than the traditional von Mises plasticity formulation, as it takes into account pressure dependent yield. Besides proving to be a better fit for cancellous bone, this crushable foam model also showed a better representation of polyurethane foam used in experimental testing.

In order to estimate bone drilling forces during orthopaedic surgeries, Lughmani et al (2015) propose a transversely isotropic elastic-plastic rate dependent model of cortical bone. In addition to this, an element removal scheme was included in the FE analysis, simulating the advancement of the drilling bit through the cortical bone. Such a model is an example of the use of increasingly complex FE models that help improve the knowledge of very specific processes.

### **3.4 Observations Regarding Constitutive Models**

Most material models described here, in particular the more recent ones, are probably too complex for the objectives of most FE studies. The choice of constitutive models depends ultimately on the type of study being performed. In a healthy human being, materials with very dissimilar mechanical behaviours are interconnected, these materials may exhibit properties, such as Young's modulus, differing by several orders of magnitude. For this reason it is paramount to adapt constitutive models to each particular analysis. If, for instance, it is the researcher's aim to analyse the behaviour of a particular joint under normal physiological loads, then it is not expected for a bone adjacent to that joint to reach yield stresses or even to have any noticeable strains; in this case, bones, without perceptible errors, can be modelled as rigid elements. If, on the other end of the spectrum, it is a requirement of the study to understand a bone's load carrying capacity, as would be the case for most orthopaedic surgeries, then the bone constitutive model should be as realistic as possible. Within this field of biomechanics where soft tissues are sometimes side by side with titanium alloys, a sensible choice of constitutive models seems imperative.

## 4. Experimental Validation

Experimental validation was not always seen as an important step in the process of assessing the quality of an FE analysis. When Brekelmans et al (1972) introduced the FE method to the field of biomechanics, it was meant to replace experimental analysis. Their intent was to affirm FE analysis as a superior tool to contemporary experimental techniques:

*“A comparison of [finite element analysis] (...) possibilities with those afforded by the experimental techniques or classical analytical theories is clearly in favour of the analysis with the aid of the finite element method.”*

Throughout their historical article, the only time they did not disregard experimental techniques was when they enumerated reasons for choosing the femur as an object of analysis:

*“The femur was chosen because (...) it is currently a focus of interest in the literature on theoretical and experimental investigations; this affords a possibility of comparing results.”*

The contempt for experimental analysis is very clear, nonetheless this sentence touched a very important aspect in the development of FE analysis that would follow: the need to somehow validate results. The more obvious and direct method was to compare them with results obtained experimentally.

Providing a background, at the beginning of their article, Brekelmans et al made a description of experimental methods existing at the time:

- Brittle coating technique: a technique that relied on the cracking of varnish previously applied to the surface of bone. The lines created by the cracked varnish when the specimens were tested would reveal deformations.
- Optical method (photo-stress technique): the bone to be analysed was subjected to a treatment that would give its surface particular optical properties. When loaded and subjected to a polarized light, lines would appear on the bone surface and conclusions could be taken.
- Strain-gauge measurements: a method that is still used today, in which strain-gauges are glued to the bone surface, and can, therefore, take direct measurements of strains in relation with known loads.
- Photo-elastic technique: a plastic model of the bone was made, it was then illuminated with polarized light, resulting in the appearance of lines in the model. Conclusions were taken in accordance with those lines.

Almost a decade later, Huiskes et al (1981) claimed to be among the first investigators to perform a well-defined comparison between theoretical and experimental results. Using both femurs of the same cadaver, they used the left one to perform experimental studies, while the right one was cut into sections in order to acquire precise dimensions. Experimental measurements were made through the application of strain-gauge rosettes, 100 in total. From the experimental results they derived two constitutive models that were applied to FE analyses. Through this process they obtained good agreement between results. Huiskes et al accepted that some discrepancies between

strain gauge and FE analysis values could result from inadequate mesh refinement, which was limited in view of computer costs at the time.

Much more recently, in an editorial paper regarding the quality of published works on FE analysis in biomechanics, Viceconti et al (2005) defined validation as:

*“The process that ensures that the numerical model accurately predicts the physical phenomenon it was design to replicate.”*

However, the authors go on to say that validating a numerical model completely is generally impossible, and compared this process to the more generalized process of science, where validation is reached through a slow procedure. Viceconti et al also warned against the clinical use of FE models not correctly interpreted and thoroughly validated, while accepting that this is a very difficult task considering the nature of biological tissues.

#### **4.1 Various Experimental Validation Techniques**

While not exactly keeping pace with FE analysis' evolution, which has been exceptional, experimental methods have also shown some development. In some instances these were very much dependent on the resources available to researchers, as is the case when cadavers are used. This method may raise some moral and availability issues in some societies, epochs, or institutions. In order to bypass these difficulties and improve results in general, many researchers have made use of their ingenuity, creating different ways to experimentally validate FE analysis.

Taylor et al (1995) validated stress values obtained in their FE analysis of a hip prosthesis femoral component by comparing with existing values of clinically measured subsidence. Values of subsidence were acquired two years after the intervention and were all for the same type of surgical hardware. This was not a straightforward validation as they compared very different parameters: stress values obtained in an FE analysis versus subsidence measured two years after surgery. Nonetheless they obtained good correlations when comparing magnitudes of those two parameters. Kumaresan et al (1999) validated their FE model of a cervical spine through data derived from experiments on eight spinal cadaver units. They collected data through a built-in force gauge and a linear variable differential transformer connected in-series to the electrohydraulic piston, an assembly that enabled recording applied force against deflection. Strain gauges were also used, glued to the anterior part of the vertebrae and the lateral masses of the middle vertebra. A correction factor was applied to account for the difference in age of the cadaver specimens used experimentally and the specimen used for the FE model.

With the objective of measuring anisotropic viscoelastic properties of cortical bone, Iyo et al (2004) collected two types of rectangular bovine femur samples: one with the long axis coinciding with the long axis of the bone and the other with the long axis coinciding with the transverse axis of the bone. These samples were subjected to three-point bending loads in saline solution at a constant temperature of 37°C. Measurements were made using a set of devices that included a strain gauge transducer used as a force sensor, and a position detector. After the initial load was applied, the reaction force produced by the bone sample was recorded as a function of time for up to 10<sup>5</sup> seconds. With values obtained it was possible to derive relaxation constitutive properties of cortical bone.

Regarding the validation of an FE analysis of a rat tibia, Evans et al (2012) used an original method which involved loading the specimen inside a micro-CT scanner. The 3D geometry of the bone

was registered unloaded and loaded using a material testing stage inside a micro-CT scanner. Hundreds of landmarks were visually marked from the surface and interior of the bone, thus comprising cortical and cancellous bone. The movement of these landmarks upon loading was quantified and compared with values obtained for the same landmarks on the FE model. This process allowed calibration of the Young's modulus of the bone as well as a qualitative validation of the FE analysis. Overall, Evans et al obtained an unrealistic Young's modulus of one to two orders of magnitude lower than expected, but the authors alleged that this might have been the result of rigid body motion and other related difficulties.

In order to estimate the fracture load of the proximal femur through a more expedite process, Koivumaki et al (2012) tested 61 human femur cadaver bones under loads simulating a side fall. Of these 61 femurs, 21 were used to define the threshold strain beyond which there was a fracture. The other 40 specimens were used to validate the FE analysis. Their study had the peculiarity of neglecting cancellous bone contribution in the overall resistance of bone.

Concerning the validation of an FE analysis of cortical bone drilling, Lughmani et al (2015) used the diaphysis of bovine femurs cut into approximately rectangular specimens. These specimens were mounted on a force transducer which measured the drilling force. The force transducer was attached to a rotating table that had its rotation restricted by a cantilever beam equipped with a strain gauge, thus providing the drilling torque. These forces were recorded at a rate of 1000 Hz by a data acquisition system. The experiments were repeated for a considerable number of specimens at varying rotations per minute applied by a DC servo motor, always using a 2.5 mm drill bit. The results showed good agreement with the FE analysis.

#### **4.2 Use of Modal Frequencies**

Taylor et al (2002) experimentally measured the modal frequencies of a femur using an apparatus comprising soft elastic straps, a unidirectional piezoelectric accelerometer fixed to the surface of the bone and an impact hammer containing a force transducer. Natural frequencies and corresponding mode shapes between 0 and 1000 Hz were recorded. An FE model of the same bone was created through CT scan imaging, and an orthotropic elastic constitutive model was calibrated in order to achieve the same modal frequencies and shapes. In a final step, the properties of the bone were measured using transmission ultrasound techniques, which revealed good correlation with FE analysis results.

Also using modal analysis to choose the best fit constitutive model, Scholz et al (2013) compared the experimentally measured frequencies on ten human pelvic bone specimens with those obtained in FE analysis using the specimens' geometry. Scholz et al used the experimental results from Neugebauer et al (2011), who used a 3D laser vibrometer to obtain the resonating frequencies between 100 and 2000 Hz of the ten specimens. The setup consisted of three measuring laser heads, two aluminium rivets for suspending the bone, a force sensor connected through an aluminium plate, and eight markers attached to the bone for geometric referencing. Comparison between FE analysis and experimental observation showed that even the constitutive model providing the closest results, still produced lower resonance frequencies, indicating that FE models lacked stiffness.



### 4.3 Use of Synthetic Bone

The use of human cadaver bones poses several problems, an alternative in biomechanical studies is the use of artificial bones. These synthetic structures try to reproduce natural bones' mechanical properties with the added advantage of being more constant. Known advantages of artificial bones over natural human bones include: less geometric and mechanical variability, greater availability, easier to handle and to preserve (Cristofolini, et al., 1996). For these reasons several authors have opted for using artificial bones instead of natural bones in their studies.

In order to validate FE analyses of the distal femur part of total knee replacements, Completo et al (2007) used synthetic bones to replicate three different reconstruction techniques. Strains were measured on ten different locations of the bone using rosette strain gauges, which were connected to a computer. Two different load cases simulating physiological activities were applied by means of a pneumatic device, and were repeated five times. Overall good agreement was reached between averaged experimentally obtained strain values and FE analysis values.

Also using synthetic bones, in this case tibiae, Nelly et al (2013) performed an experimental and FE analysis study to determine the influence of cancellous bone plasticity during press-fit implantation of a tibial component in total knee arthroplasty. They used seven specimens, in which the distal part was potted while the implant was being driven into the proximal part of the tibiae by means of a testing machine that simultaneously recorded loads applied at a prescribed displacement rate. Preceding implant insertion, a hole of 11 mm diameter was punched through the artificial cancellous bone. As the implant tapered from 12 to 10 mm diameter, it caused an interference fit of 1 mm in the proximal part. With the objective of accurately simulating the artificial cancellous bone, Nelly et al also performed uniaxial compression tests on cubic samples of the same polyurethane material used in the artificial tibiae. These experiments were used to validate an FE analysis simulating the same press-fit implantation.

Regarding the validation of an FE analysis on a patellofemoral arthroplasty, Castro et al (2015) used the experimental results from Meireles et al (2010) for the same procedure. Meireles et al used five synthetic femurs and a tibia. Five triaxial rosette strain gauges were glued to the femurs, and were connected to a data acquisition system, which was itself connected to a computer. The joint was tested in a testing machine under various loading conditions simulating daily activities in the intact condition and in the post-surgery state. The readings obtained from the strain gauges showed good agreement with the FE analysis performed by Castro et al. Some differences were attributed to difficulties related with reproducing the exact location of load application and strain gauges on the FE model.

### 4.4 Use of Strain Gauges

The use of strain gauges is not a novelty (Brekelmans, et al., 1972), but with some improvements throughout the last decades, they have remained instruments of choice to many researchers. In many cases they were used in conjunction with other techniques, e.g. (Kumaresan, et al., 1999). In other cases they were the main means of information acquisition. Strain gauges have some known limitations such as only being capable of recording information from the location they are attached to, they can only be used on the surface, and they can disturb the specimens being tested. Nonetheless, the information collected by these instruments is sometimes sufficient to help validate FE analysis.

In order to estimate the accuracy of a simplified constitutive model, Taddei et al (2006) performed several experiments on a human cadaver femur. A total of thirteen rosette strain gauges were glued to the bone. The specimen was tested on a material-testing machine in several configurations that covered a physiological range of loads corresponding to normal activities, including walking, single leg stance, stair climbing and others. Strains were recorded during the different loading processes and after load removal for a period of 90 seconds. Each load configuration was repeated five times and the bone was kept moist by wrapping it in cloths soaked with a saline solution. With the objective of determining which density-elasticity relationship best fitted the mechanical properties of the ulna, Austman et al (2008) compared experimentally obtained strain values with values acquired through the application of six different constitutive model equations found in the literature. They glued 12 uniaxial strain gauges to six different locations on eight ulna specimens. Loads were applied by means of a materials testing machine and respective strains recorded. In the FE models, the elements located under each strain gauge were identified and their strain values averaged. This allowed a direct comparison between experiment and all six FE analysis that allowed the evaluation of each constitutive model, leading Austman et al to identify the two best matches.

#### **4.5 Use of Optical Recording Devices**

A more recent method of measuring strains and strain rates has been the use of optical recording devices. These type of devices encompass many different instruments of differing complexities, from simple cameras to 3D laser measuring tools. Regardless of form, their objective is to follow the location of specific points as a function of time and applied load. In many cases landmarks are glued or otherwise attached to the specimen being tested, so that movements are more easily recorded. In some studies they are the only means through which strains are recorded. When correctly applied, this type of methods is capable of obtaining a more comprehensive recording of strains and displacements than other methods limited to discrete position readings.

#### **4.6 Measurement of Micro-motions Between Implant and Bone**

With the objective of estimating micromotions between a femur and a hip stem after implantation, Abdul-Kadir et al (2008) replicated the surgical insertion in four femur cadaver specimens. Through two holes in the bone, two points in the hip stem were marked with a linear variable differential transducer (LVDT), one in the proximal part and the other in the distal part. Using a universal materials testing machine, micromotions between the hip stem and the femur upon loading and unloading were visually measured. An FE model of bone and implant using CT scans was created that could afterwards be validated by the previously made experimental investigation. Also intending to measure micromotions after insertion of an implant, Chong et al (2010) also used LVDTs on a tibia following total knee replacement. In this case the measurements were taken between the implant tray edge and the adjacent supporting bone at three different locations. Three load sequences were performed with intervening unloading periods, and the micromotions obtained were averaged and used to validate a corresponding FE analysis

## 5. Discussion

Bone finite element analysis poses a series of additional difficulties comparing with other structural or mechanical fields. As it is hopefully noticeable on the descriptions made throughout this chapter, there is a lot of variability of mechanical behaviours between anatomical parts. As described above, a single bone can be represented using multiple constitutive laws. Further to this variability, there is another issue that has been increasingly present on researchers' minds: inter-patient variability, e.g.: (Viceconti, et al., 2004), (Weiss, et al., 2005), (Laville, et al., 2009), (Rothstock, 2010), (Niemeyer, et al., 2012), (Taylor, et al., 2013), (Pankaj, 2013), (Arregui-Mena, et al., 2014), (Amirouche, 2014), (Taylor & Prendergast, 2015). FE analyses are performed for well-defined geometries, constitutive laws and boundary conditions, there is no way that a single FE analysis can account for anatomical differences between patients. This is, perhaps, where the frontier presently lies for this technique. Despite their complexity, there are already constitutive models suitably describing the mechanical behaviour of bony tissues. For most studies, researchers do not even need to use the most complicated version of these models, as simpler models will suffice. Errors of interpretation of results may emerge from the lack of validation from a big enough sample in order to have high levels of confidence. During experimental validation, when using cadaver specimens, researchers know that the bigger the sample size the higher the assurance they can get from the process. In a similar fashion, the FE method is also developing in order to account for patient variability and patient specific analysis. With improving image technology, computer power and process automation, FE can continue contributing in the development of diagnoses and surgical techniques.

**Acknowledgements** This work is supported by the project POCI-01-0145-FEDER-028424 – PTDC/EME-SIS/28424/2017, funded by Programa Operacional Competitividade e Internacionalização (COMPETE 2020) on its component FEDER and by funding from FCT—Fundação para a Ciência e Tecnologia on its component OE.

## 6. References

- Abdul-Kadir, M. et al., 2008. Finite element modelling of primary hip stem stability: The effect of interference fit. *J. Biomech.*, Volume 41, pp. 587-594.
- Adams, J., 2009. Quantitative computed tomography. *Europ. J. Radiol.*, Volume 71, pp. 415-424.
- Amirouche, F. e. a., 2014. Factors influencing initial cup stability in total hip arthroplasty. *Clin. Biomech.*, Volume 29, pp. 1177-1185.
- Arregui-Mena, J., Margetts, L. & Mummery, P., 2014. Practical application of the stochastic finite element method. *Comp. Meth. Eng.*, pp. DOI 10.1007/s11831-014-9139-3.
- Ascenzi, A., 1993. Biomechanics and Galileo Galilei. *J. Biomech.*, 26(2), pp. 95-100.
- Austman, R., Milner, J., Holdsworth, D. & Dunning, C., 2008. The effect of the density-modulus relationship selected to apply material properties in a finite element model of long bone. *J. Biomech.*, Volume 41, pp. 3172-3176.
- Beillas, P., Lee, S., Tashman, S. & Yang, K., 2007. Sensitivity of the tibio-femoral response to finite element modeling parameters. *Comp. Meth. Biomech. Biomed. Eng.*, 10(3), pp. 209-221.
- Bendjaballah, M., Shirazi-Adl, A. & Zukor, D., 1995. Biomechanics of the human knee joint in compression: reconstruction, mesh generation and finite element analysis. *The Knee*, 2(2), pp. 69-79.
- Bowden, A. et al., 2008. Quality of motion considerations in numerical analysis of motion restoring implants of the spine. *Clin. Biomech.*, Volume 23, pp. 536-544.

Brekelmans, W., Poort, H. & Slooff, T., 1972. A new method to analyse the mechanical behavior of skeletal parts. *Acta Orthop. Scand.*, Volume 43, pp. 301-317.

Brown, T. & Ferguson, A., 1980. Mechanical property distributions in the cancellous bone of the human proximal femur. *Acta Orthop. Scand.*, Volume 51, pp. 429-437.

Burkhart, T., Andrews, D. & Dunning, C., 2013. Finite element modeling mesh quality, energy balance and validation methods: A review with recommendations associated with the modeling of bone tissue. *J. Biomech.*, Volume 46, pp. 1477-1488.

Carnelli, D. e. a., 2010. A finite element model for direction-dependent mechanical response to nanoindentation of cortical bone allowing for anisotropic post-yield behaviour of the tissue. *J. Biomech. Eng.*, Volume 132, pp. 081008.1-081008.10.

Carnelli, D. e. a., 2011. Nanoindentation testing and finite element simulations of cortical bone allowing for anisotropic elastic and inelastic mechanical response. *J. Biomech.*, Volume 44, pp. 1852-1858.

Carter, D. & Hayes, W., 1976. Bone compressive strength: the influence of density and strain rate. *Science*, Volume 194, pp. 1174-1175.

Carter, D. & Hayes, W., 1977. The compressive behaviour of bone as a two-phase porous structure. *J. Bone Joint Surg.*, pp. 954-962.

Castro, A., Completo, A., Simões, J. & Flores, P., 2015. Biomechanical behaviour of cancellous bone on patellofemoral arthroplasty with Journey prosthesis: a finite element study. *Comp. Meth. Biomech. Biomed. Eng.*, 18(10), pp. 1090-1098.

Chang, W. e. a., 1999. Uniaxial yield strains for bovine trabecular bone are isotropic and asymmetric. *J. Orthop. Res.*, Volume 17, pp. 582-585.

Chong, D., Hansen, U. & Andrew, A., 2010. Analysis of bone-prosthesis interface micromotion for cementless tibial prosthesis fixation and the influence of loading conditions. *J. Biomech.*, Volume 43, pp. 1074-1080.

Completo, A., Fonseca, F. & Simões, J., 2007. Experimental validation of intact and implanted distal femur finite element models. *J. Biomech.*, Volume 40, pp. 2467-2476.

Cowin, S. C., 2001. *Bone mechanics handbook*. 2nd ed. s.l.:CRC Press.

Cristofolini, L., Viceconti, M., Cappello, A. & Toni, A., 1996. Mechanical validation of whole bone composite femur models. *J. Biomech.*, 29(4), pp. 525-535.

Dempster, W. & Liddicoat, R., 1952. Compact bone as a non-isotropic material. *Amer. J. Anat.*, 91(3), pp. 331-362.

Denozière, G. & Ku, D., 2006. Biomechanical comparison between fusion of two vertebrae and implantation of an artificial intervertebral disc. *J. Biomech.*, Volume 39, pp. 766-775.

Donahue, T., Hull, M., Rashid, M. & Jacobs, C., 2003. How the stiffness of meniscal attachments and meniscal material properties affect tibio-femoral contact pressure computed using a validated finite element model of the human knee joint. *J. Biomech.*, Volume 36, pp. 19-34.

Donald, B., 2011. *Practical Stress Analysis With Finite Elements*. 2nd ed. Dublin: Glasnevin Publishing.

Dong, L. et al., 2013. Development and validation of a 10-year-old child ligamentous cervical spine finite element model. *A. Biomed. Eng.*, 41(12), pp. 2538-2552.

Evans, S. et al., 2012. Finite element analysis of a micromechanical model of bone and a new approach to validation. *J. Biomech.*, Volume 45, pp. 2702-2705.

Ezquerro, F. et al., 2011. Calibration of the finite element model of a lumbar functional spinal unit using an optimization technique based on differential evolution. *Med. Eng. Phys.*, Volume 33, pp. 89-95.

Faizan, A. et al., 2009. Do design variations in the artificial disc influence cervical spine biomechanics? A finite element investigation. *Eur. Spine J.*, 21(Suppl. 5), pp. S653-S662.

Galante, J., Rostoker, W. & Ray, R., 1970. Physical properties of trabecular bone. *Calc. Tiss. Res.*, Volume 5, pp. 236-246.

Gu, K. & Li, L., 2011. A human knee joint model considering fluid pressure and fiber orientation in cartilages and menisci. *Med. Eng. Phys.*, Volume 33, pp. 497-503.

Hodgkinson, R. & Currey, J., 1992. Young's modulus, density and material properties in cancellous bone over a large density range. *J. Mat. Scien. Mat. Med.*, Volume 3, pp. 377-381.

Huiskes, R. & Chao, E., 1983. A survey of finite element analysis in orthopedic biomechanics: the first decade. *J. Biomech.*, 16(6), pp. 385-409.

Huiskes, R., Janssen, J. & Slooff, T., 1981. A detailed comparison of experimental and theoretical stress-analyses of a human femur. *Mech. Proper. Bone*, Volume 45, pp. 211-234.

Hussain, M. et al., 2012. Corpectomy versus discectomy for the treatment of multilevel cervical spine pathology: a finite element model analysis. *Spine J.*, Volume 12, pp. 401-408.

Iyo, T. e. a., 2004. Anisotropic viscoelastic properties of cortical bone. *J. Biomech.*, Volume 37, pp. 1433-1437.

Kalender, W. et al., 1995. The European Spine Phantom – a tool for standardization and quality control in spinal bone mineral measurements by DXA and QCT. *Eur. J. Radiol.*, Volume 20, pp. 83-92.

Kinzl, M., Wolfram, U. & Pahr, D., 2013. Identification of a crushable foam material model and application to strength and damage prediction of human femur and vertebral body. *J. Mech. Beha. Biom. Mat.*, Volume 26, pp. 136-147.

Koivumaki, J. e. a., 2012. Cortical bone finite element models in the estimation of experimentally measured failure loads in the proximal femur. *Bone*, Volume 51, pp. 737-740.

Kopperdahl, D. & Keaveny, T., 1998. Yield strain behaviour of trabecular bone. *J. Biomech.*, Volume 31, pp. 601-608.

Kumaresan, S., Yoganandan, N., Pintar, F. & Maiman, D., 1999. Finite element modeling of the cervical spine: role of the intervertebral disc under axial and eccentric loads. *Med. Eng. Phys.*, Volume 21, pp. 689-700.

Laville, A., Laporte, S. & Skalli, W., 2009. Parametric and subject-specific finite element modelling of the lower cervical spine. Influence of geometrical parameters on the motion patterns. *J. Biomech.*, Volume 42, pp. 1409-1415.

Laz, P. et al., 2007. Incorporating uncertainty in mechanical properties for finite element-based evaluation of bone mechanics. *J. Biomech.*, Volume 40, pp. 2831-2836.

Li, L., Cheung, J. & Herzog, W., 2009. Three-dimensional fibril-reinforced finite element model of articular cartilage. *Med. Biol. Eng. Comput.*, Volume 47, pp. 607-615.

Little, J. & Adam, C., 2011. Effects of surgical joint destabilization on load sharing between ligamentous structures in the thoracic spine: A finite element investigation. *Clin. Biomech.*, Volume 26, pp. 895-903.

Liu, S. e. a., 2010. High-resolution peripheral quantitative computed tomography can assess microstructural and mechanical properties of human distal tibial bone. *J. Bone Min. Res.*, 25(4), pp. 746-756.

Liu, S. e. a., 2014. Effect of bone material properties on effective region in screw-bone model: an experimental and finite element study. *Biomed. Eng. Onl.*, p. 13:83.

Lotz, J., Gerhart, T. & Hayes, W., 1990. Mechanical properties of trabecular bone from the proximal femur: a quantitative CT study. *J. Comp. Assist. Tomogr.*, Volume 14, pp. 107-114.

Lughmani, W., Marouf, K. & Ashcroft, I., 2015. Drilling in cortical bone: a finite element model and experimental investigations. *J. Mech. Beha. Biom. Mat.*, Volume 42, pp. 32-42.

Marangalou, J. e. a., 2013. A novel approach to estimate trabecular bone anisotropy using a database approach. *J. Biomech.*, Volume 46, pp. 2356-2362.

Meireles, S., Completo, A., Simões, J. & Flores, P., 2010. Strain shielding in distal femur after patellofemoral arthroplasty under different activity conditions. *J. Biomech.*, Volume 43, pp. 477-484.

Moglo, K. & Shirazi-Adl, A., 2003. On the coupling between anterior and posterior cruciate ligaments, and knee joint response under anterior femoral drawer in flexion: a finite element study. *Clin. Biomech.*, Volume 18, pp. 751-759.

Morgan, E., Bayraktar, H. & Keaveny, T., 2003. Trabecular bone modulus-density relationships depend on anatomic site. *J. Biomech.*, Volume 36, pp. 897-904.

Morgan, E. & Keaveny, T., 2001. Dependence of yield strain of human trabecular bone on anatomical site. *J. Biomech.*, Volume 34, pp. 569-577.

Mow, V. & Huiskes, R., 2005. *Basic Orthopaedic Biomechanics and Mechano-Biology*. 3rd ed. Philadelphia: Lippincott Williams & Wilkins.

Nazemi, S. et al., 2015. Prediction of proximal tibial subchondral bone structural stiffness using subject-specific finite element modelling: Effect of selected density-modulus relationship. *Clin. Biomech.*, Volume 30, pp. 703-712.

Nelly, N. e. a., 2013. An investigation of the inelastic behaviour of trabecular bone during the press-fit implantation of a tibial component in total knee arthroplasty. *Med. Eng. Phys.*, Volume 35, pp. 1599-1606.

Neugebauer, R. et al., 2011. Experimental modal analysis on fresh-frozen human hemipelvic bones employing a 3D laser vibrometer for the purpose of modal parameter identification. *J. Biomech.*, Volume 44, pp. 1610-1613.

Niemeyer, F., Wilke, H. & Schmidt, H., 2012. Geometry strongly influences the response of numerical models of the lumbar spine - A probabilistic finite element analysis. *J. Biomech.*, Volume 45, pp. 1414-1423.

Pancanti, A., Bernakiewicz, M. & Viceconti, M., 2003. The primary stability of a cementless stem varies between subjects as much as between activities. *J. Biomech.*, Volume 36, pp. 777-785.

Pankaj, P., 2013. Patient-specific modelling of bone and bone-implant systems: the challenges. *J. Numer. Methods Biomed. Eng.*, 29(2), pp. 233-249.

Papaioannou, G. et al., 2008. Patient-specific knee joint finite element model validation with high-accuracy kinematics from biplane dynamic Roentgen. *J. Biomech.*, Volume 41, pp. 2633-2638.

Parr, W. et al., 2013. Finite element micro-modelling of a human ankle bone reveals the importance of the trabecular network to mechanical performance: New methods for generation and comparison of 3D models. *J. Biomech.*, Volume 46, pp. 200-205.

Peña, E., Calvo, B., Martínez, M. & Doblaré, M., 2006. A three-dimensional finite element analysis of the combined behavior of ligaments and menisci in the healthy human knee joint. *J. Biomech.*, Volume 39, pp. 1686-1701.

Ramaniraka, N., Terrier, A., Theumann, N. & Siegrist, O., 2005. Effects of the posterior cruciate ligament reconstruction on the biomechanics of the knee joint: a finite element analysis. *Clin. Biomech.*, Volume 20, pp. 434-442.

Rho, J., Hobatho, M. & Ashman, R., 1995. Relations of mechanical properties to density and CT numbers in human bone. *Med. Eng. Phys.*, Volume 17, pp. 347-355.

Rietbergen, B. & Ito, K., 2015. A survey of micro-finite element analysis for clinical assessment of bone strength: The first decade. *J. Biomech.*, Volume 48, pp. 832-841.

Rohlmann, A., Boustani, H., Bergmann, G. & Zander, T., 2010. Effect of a pedicle-screw-based motion preservation system on lumbar spine biomechanics: A probabilistic finite element study with subsequent sensitivity analysis. *J. Biomech.*, Volume 43, pp. 2963-2969.

Rothstock, S. e. a., 2010. Primary stability of uncemented femoral resurfacing implants for varying interface parameters and material formulations during walking and stair climbing. *J. Biomech.*, Volume 43, pp. 521-526.

Schmidt, H., Galbusera, F., Rohlmann, A. & Shirazi-Adl, A., 2013. What have we learned from finite element model studies of lumbar intervertebral discs in the past four decades?. *J. Biomech.*, Volume 46, pp. 2342-2355.

Schmidt, H. et al., 2007. Application of a calibration method provides more realistic results for a finite element model of a lumbar spinal segment. *Clin. Biomech.*, Volume 22, pp. 377-384.

Scholz, R. e. a., 2013. Validation of density-elasticity relationships for finite element modelling of human pelvic bone by modal analysis. *J. Biomech.*, Volume 46, pp. 2667-2673.

Taddei, F. et al., 2006. Subject-specific finite element models of long bones: An in vitro evaluation of the overall accuracy. *J. Biomech.*, Volume 39, pp. 2457-2467.

Taddei, F., Pancanti, A. & Viceconti, M., 2004. An improved method for the automatic mapping of computed tomography numbers onto finite element models. *Med. Eng. Phys.*, Volume 26, pp. 61-69.

Taylor, M., Bryan, R. & Galloway, F., 2013. Accounting for patient variability in finite element analysis of the intact and implanted hip and knee: a review. *Int. J. Numer. Methods Biomed. Eng.*, 29(2), pp. 273-292.

Taylor, M. e. a., 1995. Cancellous bone stresses surrounding the femoral component of a hip prosthesis: an elastic-plastic finite element analysis. *Med. Eng. Phys.*, Volume 17, pp. 544-550.

Taylor, M. & Prendergast, P., 2015. Four decades of finite element analysis of orthopaedic devices: Where are we now and what are the opportunities. *J. Biomech.*, Volume 48, pp. 767-778.

Taylor, W. e. a., 2002. Determination of orthotropic bone elastic constants using FEA and modal analysis. *J. Biomech.*, Volume 35, pp. 767-773.

Viceconti, M., Davinelli, M., Taddei, F. & Cappello, A., 2004. Automatic generation of accurate subject-specific bone finite element models to be used in clinical studies. *J. Biomech.*, Volume 37, pp. 1597-1605.

Viceconti, M., Olsen, S. & Burton, K., 2005. Extracting clinically relevant data from finite element simulations. *Clin. Biomech.*, Volume 20, pp. 451-454.

Wang, W., Zhang, H., Sadeghipour, K. & Baran, G., 2013. Effect of posterolateral disc replacement on kinematics and stress distribution in the lumbar spine: A finite element study. *Med. Eng. Phys.*, Volume 35, pp. 357-364.

Weiss, J. et al., 2005. Three-dimensional finite element modeling of ligaments: Technical aspects. *Med. Eng. Phys.*, Volume 27, pp. 845-861.

Wirtz, D. et al., 2000. Critical evaluation of known bone material properties to realize anisotropic FE-simulation of the proximal femur. *J. Biomech.*, Volume 33, pp. 1325-1330.

Wolfram, U., Wilke, H. & Zysset, P., 2010. Valid finite element models of vertebral trabecular bone can be obtained using tissue properties measured with nanoindentation under wet conditions. *J. Biomech.*, Volume 43, pp. 1731-1737.

Yue-fu, D. et al., 2011. Accurate 3D reconstruction of subject-specific knee finite element model to simulate the articular cartilage defects. *J. Shang. Jiaot. Univ. (Sci.)*, 16(5), pp. 620-627.

Zander, T., Rohlmann, A., Calisse, J. & Bergmann, G., 2001. Estimation of muscle forces in the lumbar spine during upper-body inclination. *Clin. Biomech.*, 16(1), pp. S73-S80.

Zhang, J., Wang, F. & Zhou, R. X. Q., 2011. A three-dimensional finite element model of the cervical spine: an investigation of whiplash injury. *Med. Biol. Eng. Comput.*, Volume 49, pp. 193-201.

